

The Adsorption of Full-Fat Almarei Milk Solution Produced in Saudi Arabia on the Surface of Flavylum Cations of Anthocyanins from Grape Peel, Red Cabbage, and Pomegranate Peel as Natural Adsorbents

Fatima A. Al-Qadri*, Raiedhah Alsaiani, Mabkhoot Alsaiani, Iman Mohammad Shedaiwa, Mervate Mohamed Mohamed and Esraa Mohamed Musa

Department of Chemistry of Sharourah's Science and Art faculty, Najran University, Saudi Arabia.
fatimaalqadri@gmail.com*

(Received on 29th March 2021, accepted in revised form 8th October 2021)

Summary: Almarei milk is produced in Saudi Arabia from aqueous solutions; this study investigates its adsorption behavior pertaining to three types of anthocyanin pigments that are used as natural food colorants and adsorbents. The three anthocyanin pigments were extracted from red cabbage (RC), grape peel (GP), and pomegranate peel (PP). The initial dye concentrations were 10–50 mg/L and temperature of the solution was 35 °C. For an equilibrium isotherms and kinetic data were evaluated using the adsorption isotherms models such as Freundlich and Langmuir models. The results which were recorded show that the best adsorption model fit with the experimental data was Langmuir model in contrast with the Freundlich model. Also more suitable adsorption kinetics model was pseudo-second order and intraparticle diffusion models than the first-order reactions. An exothermic nature was found from the results of thermodynamic adsorption for each of thermodynamic parameters like entropy (S°), (H°) enthalpy, and free energy (G°).

Introduction

Foods that are rich in phenols and consumed day by day have been found to reduce diseases like cancer and cerebrovascular mortality [1]. Red fruits such as grapes, pomegranate juice, and red cabbage are important sources of active antioxidant phenolics. Recently, foods such as these are being preferred to be used as safe, natural additives [2]. For example, the biological properties of pomegranate makes it a suitable natural food colorant [3]. Fruits and vegetables of specific colors, viz. purple, red, and blue, are rich in anthocyanins and phenolic color, water-soluble [4], and consequently, used as food colorants and in modern medicine. Furthermore, they are used as part of traditional health regimes as they can be ingested in large doses and have a very low toxicity. They are also commercially grown for their anthocyanin content [5]. The basic structure of anthocyanins-3-O-glucoside was discovered from fruits [6]. As natural food colorants, they are considered to be among the best antioxidants; further, they demonstrate a nutraceutical, antimicrobial effect on many chronic diseases when compared with that of synthetic colorants that have negative effects on the human health, particularly, on neurological functions and behavior. Chemically, milk is a heterogeneous mixture in a complex form, which contains minerals, protein (in the form of casein), fat, salts, lactose, enzymes, and vitamins, as well as important trace elements such as copper, zinc, manganese.

Anthocyanins, which contain red dye and cations of flavylum [7] at lower value of pH solution they are steady, stable and easily soluble at a lower pH

[8]. Adsorption is an interface phenomenon and defined by measuring the concentrations at the interface and adjacent phases. Adsorption processes have been accomplished to change the color of textile products and used as a cheap and effective approach to change the color of textiles products [9]. Freeze drying is a suitable method to obtain high quality dry pigments [10]. The objective of this article is investigate the process of adsorption of full-fat Almarei milk solution produced in Saudi Arabia on the surface of anthocyanins powder and Phenolic-rich foods extracted from red cabbage (RC), grape peels (GPs), and pomegranate peels (PPs). They are used as natural food colorants for the Almarai milk solution.

Experimental

Instrumentation

A Mettler Toledo microbalance with 0.1 mg accuracy was used to weight samples. A mechanical shaking and a Blue Spin magnetic hotplate stirrer with a resolution speed control accuracy of ± 1 rpm were used to conduct the experiments of adsorption. The adsorption process was done by using batch, which was conducted in a Pyrex 100 ml flask. A Whatman filter paper of 0.5 μm pore size was used for filtration. A spectrophotometer (UV-visible Genesys 10S) was used.

Preparation of Grape Peel (GP), Red Cabbage (RC), and Pomegranate Peel (PP)

Although relatively harsh solvents, such as ethanol and methanol, can be used to extract

*To whom all correspondence should be addressed.

anthocyanin pigments from fruits and vegetables, water is an appropriate alternative that is safer and better for the environment [11]. Grapes were purchased from a local market, cleaned with distilled water, and their skins were manually peeled. Then, any excess water was squeezed from the peels; at 60 °C grape peels (GP) were dried, until stable weight obtained. Fresh red cabbage (RC) was purchased from a local market, washed in distilled water, and cut and dried at room temperature. Pomegranate peel (PP) was cut into pieces, they are cleaned by distilled water for many times until became pure from any dirt and dust, finally the sample dried at room temperature.

Extraction of Anthocyanins

The anthocyanins were extracted from a 20 g sample of each of the aforementioned fruits and vegetable using a solute and methanol, a solvent ratio of 1:10 w/w in a 200 ml beaker that was magnetically stirred for 12 h. The acidified water used in the extraction process was (0.1% HCl, with pH was 3) and fed at a rate of 30ml/min at constant pressure of 40 bar. They were then exposed to two different temperatures ranging between 110 °C and 160 °C [12]. The liquid was then extracted using the filtration paper and the resulting material was then freeze-dried for 5h [13]. Finally, these materials were milled using a mortar to obtain anthocyanins powders. They were then stored in light-proof containers until required for the study.

Preparation of Adsorbate

The adsorbate used in this study was of full-fat fresh Almarei liquid milk purchased from the local market. The characteristics and nutritional information as obtained by the producer are summarized in Table 1. Different concentrations were prepared from the stock solution using distilled water at 10, 15, 20, 30, 40, and 50 mg/l. Then, using the double beam spectrophotometer, the aqueous liquid milk solution was

calibrated (UV-visible Genesys 10S). The absorbance of the Almarei milk solution was found to be 450 nm.

Batch Adsorption Process

Samples were heated at 100 °C in an oven to obtain active centers. A solution of 50 ml was added in an Erlenmeyer conical for the adsorption experiments process and the required time was determined to reach equilibrium, in which the adsorbent surface would be completely saturated at a temperature of 35 °C and pH 4. Different concentrations of the adsorbate were prepared at concentrations of 10, 15, 20, 30, 40 and 50 mg/l. Then, 2 mg of each of the adsorbents were mixed with 50 ml of aqueous milk solution that was then shaken in a thermostatic shaker at 150 rpm at 35 °C. A solution of Almarei milk (AM) was measured before adsorption to determine the amount of milk adsorbed by GP, PP, and RC, respectively. By using UV/Visible spectrophotometer the absorbance of the milk were investigated at intervals of 10, 20, 30, 40, and 50 min until the point of equilibrium was attained. The adsorbents were then separated from the liquid using filter paper. The quantity adsorbed of Almarai milk was calculated using the following (equations no 1 and 2): [14, 15]

$$q_e = \frac{(C_0 - C_e) V}{W} \quad (1)$$

$$\text{Adsorbate uptake (\%)} = \frac{(C_0 - C_t) \times 100}{C_0} \quad (2)$$

where q_e is the amount adsorbed per gram (mg/g), C_0 is the initial concentration (mg/L), C_t is the amount of equilibrium dye conc (mg/L), V is the volume of the solution (ml), and W is the adsorbent weight (g).

Table-1: Properties of fresh Almarai milk (full fat, 250 mL)

	Size	Origin	Milk information	%DV
			Total Fat 8 g	11%
			Saturated Fat 5 g	24%
			Trans Fat 0 g	-
			Cholesterol 24 mg	8%
			Sodium 129 mg	5%
			Total Carbohydrate	5%
			Dietary Fiber 0 g	0%
			Total Sugars 12 g	
			Including Added Sugars 0 g	0%
			Protein 8 g	
			Vitamin A 750.5 IU	28%
			Vitamin D3 136.0 IU	23%
			Calcium 250.4 mg	25%
Fresh milk, full fat	250 mL	Almarai Saudi Industry		

The % daily value (DV) is the percentage of the daily limit for the specified nutrient that is represented in a serving of the food as specified by guidelines; 2000 calories a day is used for general nutrition advice.

Results and Discussion

Adsorption Equilibrium

Generally, there are three steps of the adsorption process they are explained as follows:

- The transfer of the adsorbate to the exterior part of the surface for adsorbent, away from the bulk of the solution.
- Although a small quantity of adsorbate is retained on the outer surface, the adsorbate molecules spread through the pores of the adsorbent.
- The suitable adsorption for adsorbate molecules onto the surface at the internal part which are characterized by micropores and capillary spaces.
- The final step is a fast step that leads to a state of equilibrium [16] in which the driving force of the process is adsorption close to the micropores walls [17].

The indirect method was used to measure the quantity of the adsorbed concentration before and after the experiment [18], which showed that the materials having small particles with a high surface area demonstrate excellent properties [19]. It was found that higher the concentration of the sample, larger is the surface area, which gives a higher number of adsorption sites that deliver a higher uptake of the milk [20]. The results are shown in Figs 1a, 1b, and 1c.

Fig 1 shows adsorption isotherm at the equilibrium of AM on the three foodstuffs it shows an increase at low concentrations, so it indicates a high affinity toward the solute. However, at high AM concentrations, the amounts slowly increase and become constant. This can be explained as follows:

RC: q_e increased from 12 mg/g at an AM solution concentration of 10 mg/l to the highest value of 42.01 mg/g at 20 mg/l of AM, followed by stability from 44.43 to 44.44 mg/g from 30 mg/l to 40 mg/g of AM concentration.

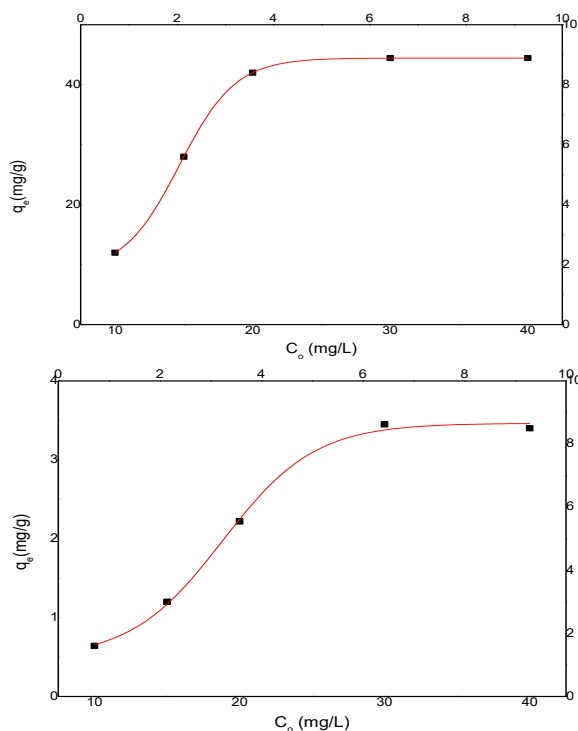
GP: q_e increased from 4.9 mg/g at a milk solution concentration of 10 mg/l to the highest value of 7.9 mg/g at 30 mg/l of milk, followed by stability from 8.1 to 8.2 mg/g from 400 mg/l to 50 mg/g AM concentration.

PP: q_e increased from 0.64 mg/g at a milk solution concentration of 10 mg/l to the highest value of 2.22 mg/g at 20 mg/l of milk, followed by stability from 3.45 to 3.44 mg/g from 30 mg/l to 40 mg/g AM concentration.

For all samples, q_e values increased when compared with those of the initial concentrations.

This is because:

- At low concentrations, the ratio between the quantities adsorbed of AM solution to the active centers that are available on the surface of adsorbents is small. This leads to the independence of fractional adsorption on the initial concentration of AM. At higher concentrations of AM, there are fewer available active centers on the adsorbent surface; therefore, the AM adsorption is dependent on the initial concentration level. Consequently, higher concentrations of AM lead to higher q_e values [21].
- At higher concentrations of AM, the gradient acts as a driving force that can solve the obstacle transfer of AM mass ions through the adsorbent solid and adsorbate liquid phases. Hence, there is a high possibility of collision between AM ions and the active sites [22]. Therefore, the increase in the adsorption of AM concentration from 20 mg/l to 40 mg/l for RC and the increase in AM concentration from 10 mg/l to 30 mg/l for GP leads to a decrease in the q_e values, as observed from the results. At high concentrations (20 mg/l for RC and 30 mg/l for GP), active adsorption sites became saturated [23] following which the q_e value decreases.



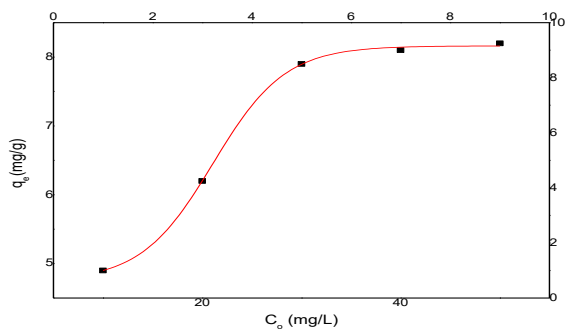


Fig. 1: The Initial concentration of the dye effect on the adsorption of Al-Mareai milk (AM) by (A) red cabbage (RC), (B) grape peel (GP), and (C) pomegranate peel (PP). (Conditions: T = 35 °C, W/V = 2 g/50 ml, time = 60 min).

The adsorption percentages listed in Table-2 show that the highest percentage adsorption of AM was on PP at 99.53%, followed by GP at 97.31%, and RC at 75.47%.

Table-2: Percentage Adsorption.

Samples	Adsorption %
Red Cabbage (RC)	75.47%
Grape Peel (GP)	97.31%
Pomegranate Peel (PP)	99.53%

Langmuir Isotherm

In this type of adsorption, the Langmuir isotherm model shows that the surface of the adsorbent consists of active centers, for monolayer adsorption and it is homogenous. The Freundlich adsorption isotherm consists of heterogeneous surfaces with multiple sites of adsorption, i.e., multilayer capacity adsorption can be achieved [24]. From The Figs of adsorption a linear line was found for Langmuir isotherm it is shown by the following equation [25]

$$\frac{C_e}{q_e} = \frac{1}{q_{max} \cdot b} + \frac{1}{q_{max}} \cdot C_e \quad (3)$$

The empirical constants of the adsorption isotherm of Langmuir would be expressed as the adsorption maximum capacity of the adsorbent, q_{max} (mg/g), and a constant related to the energy of adsorption, b (l/mg); they correspond to the energy of adsorption efficiency[26].In this study, the experiment required 60 min at 35 °C (308 K); hence, the calculation for the maximum adsorbent capacity and constants q_{max} and b is as follows: plotting C_e/q_e against q_e as shown in Fig 2 obtains a straight line. In the Langmuir adsorption model, all adsorption sites

have identical adsorption energy. The adsorption isotherm of Langmuir predicts that adsorption happened at the homogenous surface of adsorption, further explaining the existence of coverage on the adsorbate surface was monolayer at the active centers of the outer surface of the adsorbent [27]. The plot of C_e/q_e vs C_e obtains a linear trend with a slope of $1/q_e$, as shown in Fig 2. The coefficient R^2 was 0.88, 1.00, and 0.95 for RC, GP, and PP, respectively. Therefore, the adsorption of GP and PP are more suitable and fit to the Langmuir model than that of RC.

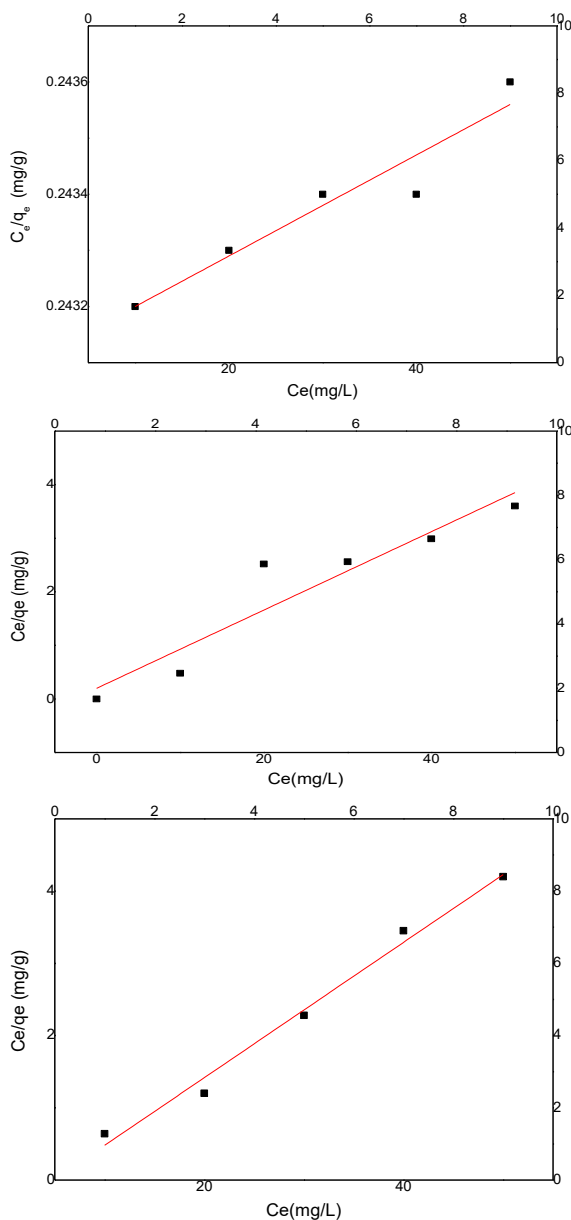


Fig. 2: Straight line of the Langmuir isotherm model for AM adsorption for (A) RC (B) GP, and (C) PP at a temperature of 302 K and pH=4.

Table-3: Langmuir and Freundlich isotherms.

Adsorbents	Langmuir isotherms			Freundlich isotherms			R2
	q max mg/mL	b mL/g	R2 mg/mL	Kf mg/mL	1/n	n mL/g	
Cabbage	11.11	0.67	0.88	1.59	0.68	7.95	0.81
Grapes	10.45	0.05	1.00	1.95	0.393	2.27	0.90
Pomegranate	1.69	2.50	0.95	1.89	1.34	0.76	0.92

The main features of the adsorption isotherm for Langmuir can be described using a special parameter, which is known as dimensionless equilibrium (R_L) [29].

$$R_L = \frac{1}{1 + bC_i} \quad (4)$$

The magnitude of R_L shows if the isotherm is favorable or non-favorable; the isotherm is undesirable when $R_L > 1$ and linear when $R_L = 1$, but if it is desirable ($0 < R_L < 1$) or irreversible ($R_L = 0$), then C_i is the initial concentration of AM (mg/L). In this study, the results were found to be 0.0086, 0.013, and 0.00041 for RC, GP, and PP, respectively. Thus, the desirable isotherm was Langmuir for the adsorption of Almarai milk for the three natural adsorbents considered in this study.

Freundlich Isotherm

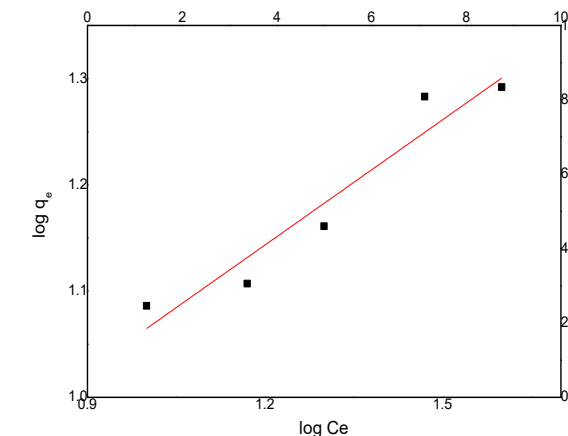
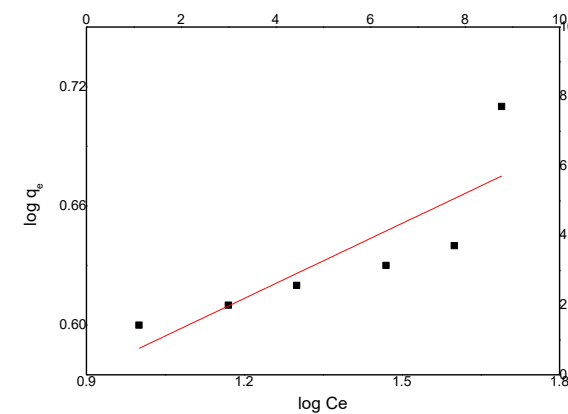
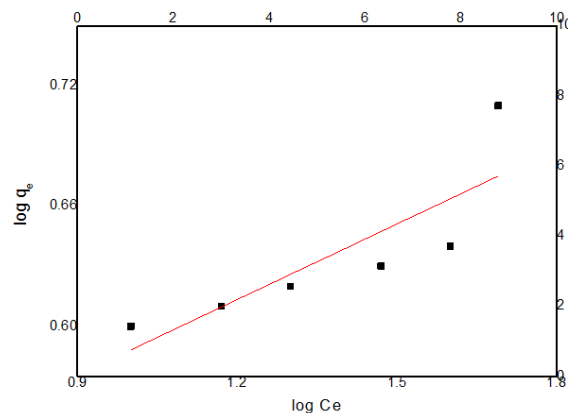
The Freundlich isotherm model is an experimental equation that shows a heterogeneous adsorbent surface and explains the possibility of the occurrence of multilayer adsorption [28]. It gives the ratio of a certain amount of the solute adsorbed by a definite weight of the adsorbent to the concentration of the solute in a solution which is not stable at various concentrations [28]. The following equations represent the logarithmic form of the Freundlich isotherm [28].

$$q_e = K_f C_e \frac{1}{n} \quad (5)$$

$$\log q_e = \log K_f + \frac{1}{n} \cdot \log C_e$$

where q_e is the equilibrium adsorbate concentration on adsorbents surfaces (mg/g), C_e is the equilibrium of the adsorbate concentration in solution (mg/l), K_f is the Freundlich constant, and n is the empirical parameter. The magnitude of n gives a measure of the favorable adsorption that occurs when the value of n is between 1 and 10 or the value of $1/n$ is less than 1; in other words, it represents that the surface of the adsorbent is heterogenous, making adsorption easy [29]. In this study, from the results of plotting a linear line was obtained of a slope of $1/n$ and intercept of

$\log K_f$ was obtained by plotting $\log q_e$ against $\log C_e$, as shown in Fig 3. The values are listed in Table-3; they indicate that the adsorptions are favorable [30].



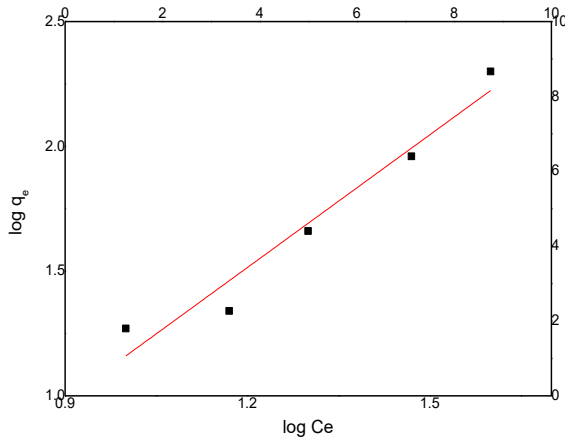


Fig. 3: Linearized Freundlich adsorption isotherm for Almaraei milk adsorption by (A) RC (B) GP, and (C) PP, at a temperature of 302 K and pH=4.

Adsorption Kinetics

The adsorption speed can be determined by two models of kinetic adsorption, viz. first and second pseudo-order reactions [31]. The equation of the first-order which is pseudo model is established, on the hypothesis that the difference of adsorption of solute with varying time depends upon the amount difference of the saturated and adsorbate uptake dosage with time [32].

First-Order Pseudo Model

Lagergren supposed the constant rate of the adsorption [33]; hence, the empirical equation used for determination pseudo first-order kinetic is written as follows:

$$\frac{dq}{dx} = K_1 (q_e - q_t) \tag{7}$$

where k_1 is the adsorption rate constant for first-order kinetic model, q_t is the quantity of adsorbed at time t (mg/g), q_e is the adsorption capacity at equilibrium (mg/g), is the amount of adsorbed at saturation at ($t = 0, q_t = 0$) and ($t = t, q = q_t$).

The linear form of the pseudo-first-order model is expressed as follows:

$$\ln(q_e - q_t) = \ln q_e - K_1 t \tag{8}$$

When $\ln (q_e - q_t)$ is plotted against t , a straight line was obtained, and rate constant k can be

evaluated from the slope, R^2 is the correlation coefficient, and theoretically, q_e can be calculated from the plot. Though a linear line was obtained from the Fig 4, and the value of $q_e, calc$ is approximately equal to the experimental value ($q_e, exp.$). However, the magnitude of R^2 was low in the first-order pseudo-kinetic model in contrast with the values obtained from the second-order pseudo-kinetic model. This is because the first-order pseudo kinetic model is a poor fit for the adsorption kinetics and it does not fit the full range of contact times. It is applied only over the initial stages through the adsorption process. The times were between 1 and 10 min [34].

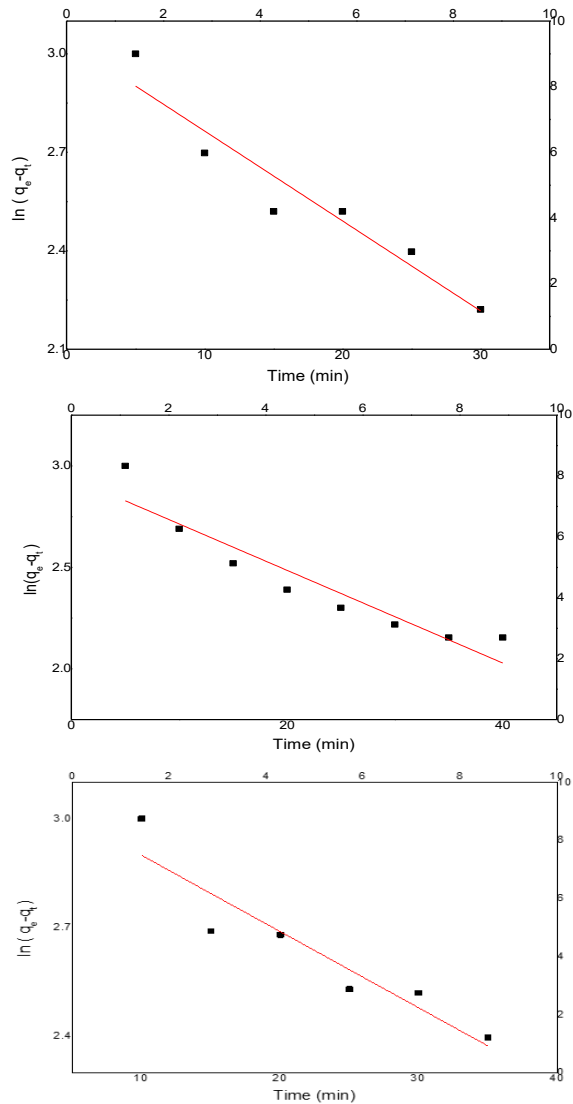


Fig. 4: The adsorption kinetics adsorption of Almaraei milk by (A) RC, (B) GP, and (C) PP at 302 K of first-order Pseudo model.

Table-4: The adsorption kinetics second-order Pseudo-and first -order Pseudo model of for Almaraei milk by (a) RC, (b) GP, and (c) PP at 302 K and pH=4.

second order Pseudo	first order Pseudo	Concentration (mg/L)		Intraparticle Diffusion Δq (%)	R2	k1 (min ⁻¹)	qe, (cal) (mg/g)	qe,(exp) (mg/g)	Adsorbents
R ₂	Δq (%)	20 mg/L							
		k ₂ (g/mg·min)	qe,(cal) (mg/g)						
0.99	0.018	0.61	3.33	2.92	0.90	0.13	3.12	3.12	Cabbage
0.95	0.08	0.91	2.5	2.66	0.87	0.11	2.90	2.91	Grapes
0.99	0.05	0.91	1.22	1.60	0.85	0.10	1.90	1.91	Pomegranate

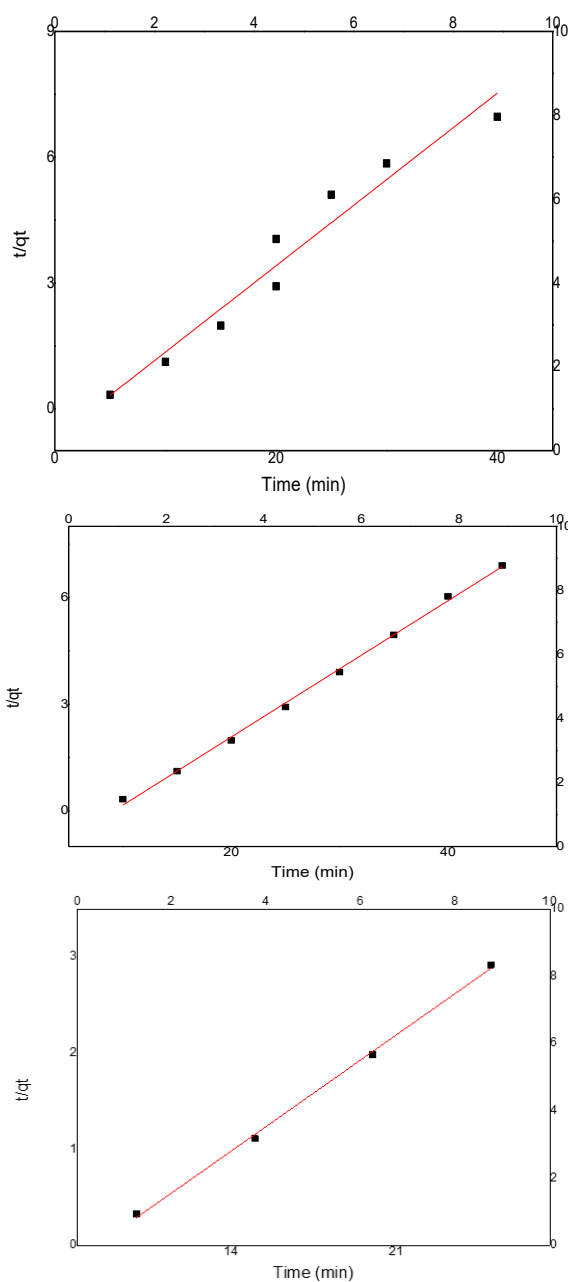


Fig. 5: The adsorption kinetics adsorption of Almaraei milk by (A) RC, (B) GP, and (C) PP at 302 K of -second-order Pseudo model.

Pseudo-second-order reaction

Second-order Pseudo kinetic model is a type of kinetic model can be utilized to determine adsorption kinetics. In this model, the interchange of electrons occurs between the adsorbent and adsorbate due to the forces of valance; in other words, it depends on a chemical reaction [35]. This model [36] is given by the following equation and estimated in the linear form at $t = 0, q = 0$ and $t = t, q = qt$:

$$\ln(q_e - q_t) = \ln q_e - K_1 t \tag{9}$$

where the rate constant of the second-order pseudo is K_2 (kps) ($g\ mg^{-1}\ min^{-1}$). of the plot t vs t/qt obtains a straight line, from which the values of K_2 and $q_{e,calc}$ values can be calculated. In this study, the results from the plot versus t/qt gives a straight line; the calculated K_2 and $q_{e,calc}$ values show that the values of $q_{e,calc}$ were approximately equal to the experimental $q_{e,exp}$ values. Furthermore, the values of coefficient R_2 for the pseudo-second-order kinetic model were found to be higher than those of the first-order pseudo kinetic model; thus, it is the best fit in describing the adsorption kinetics of AM by RC, GP, and PP. The results are shown in Fig. 5 and the analysis results are listed in Table-4.

Intraparticle

The diffusion of intraparticle model[37] was used to determine the state of the transfer and migration process for adsorption in a whiskered batch adsorption system that take place on a porous of the adsorbent surface as following:

$$q_t = k_p t^{0.5} + C \tag{10}$$

where q_t is the amount of Almarai milk adsorbed onto RC, GP, and PP at time t (mg/g) and k_p is the intraparticle diffusion that occurs on the adsorbent with a porous surface ($mg/(g \cdot min^{0.5})$), from the linear line is obtained from the plotting q_t vs $t^{0.5}$ gives a value of the rate constant for the diffusion intraparticle (mg/g .C) regarding the intensity of the border layer. Hence, if the magnitude of the intercept is larger than the effect of border layer [38], then q_t

vs $t^{0.5}$ plot obtains a straight line and the adsorption process is controlled by intraparticle diffusion. In contrast, if the linear fit exhibits multilinear curves, this indicates that two or more steps are influencing the adsorption process. If the Weber-Morris plot (q_t vs $t^{0.5}$) is found to be linear, then intraparticle diffusion take place; and if the line go through the source, then intraparticle diffusion is the only rate-limiting step [39]. In this study, a straight line was obtained by plotting q_t against $t^{0.5}$, as shown in Fig 6. As the diffusion intraparticle plots do not go through the source, that means that intraparticle diffusion and limiting-step had an important role in the adsorption. so, the processes of the adsorption obey the second-order pseudo model [40]. The results can be explained as a linear correlation owing to several steps that occurred during the adsorption process. Step one included the initial linear portions that are attributed to the initial boundary and the diffusion through the solution to the outer adsorbent surface recognized, as “the outer transfer of the mass or “film diffusion” [41]. The second step corresponded with intraparticle diffusion into the adsorbent porous [42]. The final parts horizontal of the Fig were low in speed and can be controlled by the mechanism of diffusion equilibrium [43].

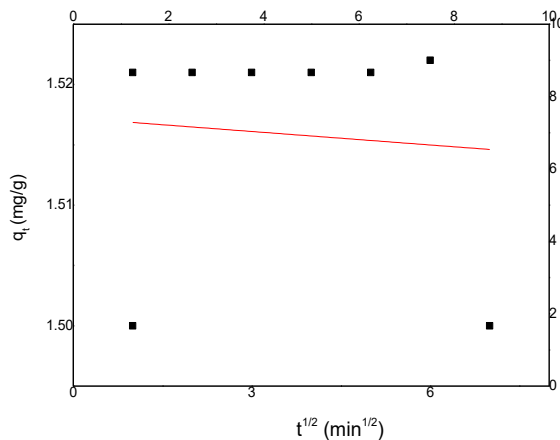
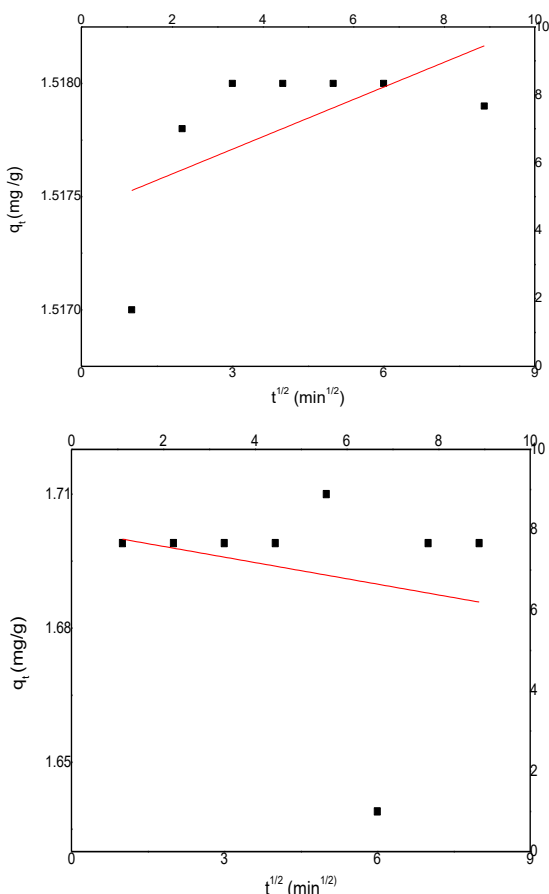


Fig. 6: The adsorption Intraparticle diffusion fit for milk onto (A) RC (B) GP and (C) PP at different initial concentrations (T=308 K, 300 rpm, and 2.0 g of adsorbent).



Testing Kinetic Validity

The validity of the models was quantitatively verified; normalized standard deviation Δq_e (%) was calculated using the equation written as follows (Anwar et. al., 2010, Njoku et. al., 2014).

$$\Delta q_e (\%) = \sqrt{\frac{\sum [(q_{e,exp} - q_{e,calc}) / q_{e,exp}]^2}{n - 1}} \quad (11)$$

where n is the number of data points, $q_{e,exp}$ is the experimental value (mg/g), and $q_{e,calc}$ is the calculated q_e from the models (mg/g). These values are listed in Table 4. The pseudo-second-order kinetic model yielded the lowest Δq_e (%) for the three adsorbents and is therefore the best model to describe the adsorption of Almarai milk onto RC, GP, and PP. The Δq_e (%) values obtained from intraparticle diffusion models reveal that those from the second-order pseudo were, little than those obtained from the first-order pseudo model. This explains that the adsorption of AM onto the three natural adsorbents is determined well by the second order pseudo kinetic model owing to the higher correlation coefficient and a big agreement between the experimental and calculated q_e values.

Adsorption Thermodynamics Parameters

The thermodynamic parameters are described using the following standard parameters: enthalpy (H°), entropy (S°), and free energy (G°). The thermodynamic parameters are described using the

following standard parameters: enthalpy (H°), entropy (S°), and free energy (G°), because of the solute in mole movement and transport from the bulk solution at the interface liquid–solid, they were calculated by Vant–Hoff equations [44].

$$\Delta G^\circ = -RT \ln K_d \quad (12)$$

$$\Delta G^\circ = \Delta H^\circ - T\Delta S^\circ \quad (13)$$

where R is the universal gas constant (8.314 J/mol.K), T is the absolute temperature (K), and K_c is the linear adsorption distribution coefficient defined as: $K_d = C_e / C_0$, where C_e is the amount adsorbed on solid at equilibrium (mg/l) and C_0 is the equilibrium concentration or the initial adsorbate concentrations and adsorbate concentrations remained in the liquid phase at equilibrium (mg/l), respectively, ΔG° is the free energy of adsorption, ΔH° is the enthalpy change (kJ/mol), and ΔS° is the entropy change (J/mol.K). From Table 5 the data results of the thermodynamic parameters expose The value of ΔH° which was negative indicates the exothermic reaction of adsorption process, while the ΔS° negative value indicates the associative mechanism of adsorption reaction which is involved during the adsorption process. The adsorption was ordered through the formation of an activated complex between adsorbate and adsorbent [45]. on the other side the positive or negative sign of ΔS° indicates the non-organized randomness of order of the adsorbate at the solid/solution interface during the adsorption: less random if $\Delta S^\circ < 0$ or more random if $\Delta S^\circ > 0$ [46]; the negative ΔS value shows decrease in the degree of freedom of the adsorbate ions in the solution. The ΔG° values were positive for all these adsorbents, which means that the adsorption reaction was non-spontaneous. Further, at high temperatures, the process of adsorption is inversely proportional to the temperature

Table-5: Adsorption Thermodynamic parameters of Almarai milk onto RC, GP, and PP

Adsorbents	ΔG° (kJ/mol)	ΔH° (kJ/mol)	ΔS° (J/mol · K)	TK
RC	3654.13	-3652.88	-11.86	303
GP	9771.67	-9769.76	-31.72	303
PP	7569.46	-7569.40	-24.57	303

Conclusions

The aim of this study was the adsorption of aqueous Almarai milk solutions on RC, GP, and PP powders. The results of data obtained show that best suitable adsorption model was Langmuir isotherm model more than Freundlich isotherms. Additionally, adsorption kinetics showed a second -order model

more suitable than the first order reaction. The results of thermodynamic parameters ΔG° , ΔS° , and ΔH° reveal the exothermic reaction for the adsorption process, and the negative values of ΔH° and ΔS° shows that in the adsorptive order, intraparticle diffusion is not the sole rate-controlling step. The adsorbents tested in this study, which are widely available, inexpensive, and easy to prepare, had a higher capacity for adsorbing AM than other natural adsorbents. Therefore, approximately 1.0 g/100 ml of food colorants is required.

Acknowledgments

Authors would like to express their gratitude to the Ministry of Education and Deanship of Scientific Research, Najran University, Kingdom of Saudi Arabia for support under code number (NU-/SERC/10/577).

Data availability

The authors will provide the data from the research, and it will be available in the article is accepted for publication.

References

1. S. K. Wong, K. Y. Chin, F. H. Suhaimi, F. Ahmad, So. I. Nirwana Effects of metabolic syndrome on bone mineral density, histomorphometry and remodelling markers in male rats, *PLoS ONE*, **13**, 0192416 (2018).
2. E. G. Beneytez, E. Revilla, F. Cabello, Ant pathocyaninern of several red grape cultivars and wines made from them. *Eur. Food. Res. Tech.*, **215**, 32 (2002).
3. Cano-Lamadrid M, Trigueros L, Marina Wojdyło, Cano-Lamadr Lorena Triguerosid, Aneta Wojdyło, Angel A Carbonell-Barrachina, Esther Sendra, Anthocyanins decay in pomegranate enriched fermented milks as a function of bacterial strain and processing conditions. *LWT-Food Sci Technol.* **80**: 193 (2017).
4. J. M. Bueno, P. S. Plaza, F. R. Escudero, A. M. Jiménez, R Fett, A. G. Asuero. Analysis and antioxidant capacity of anthocyanin pigments. Part II: chemical structure, color and intake of anthocyanins. *Crit. Rev. Anal. Chem.*, **42**, 151 (2012).
5. P. Bridle, C. F Timberlake. Anthocyanins as natural food colors—selected aspects. *Food Chem.*, **58**, 109 (1997).

6. O. M Andersen, M. Jordheim. The anthocyanins. In *Flavonoids: Chemistry, Biochemistry and Applications*. Andersen OM, Markham KR. (Eds.), Boca Raton, FL: Taylor and Francis, **551** (2006).
7. A. B. Barczak, Acylated anthocyanins as stable, natural food colorants – A review. *Pol. J. Food Nutr. Sci.*, **14**, 107 (2005).
8. H. A. Schroeder, The trace elements and nutrition. London: Faber and Faber. W. H. O. Trace elements in human. Who Technical Report Series, No. **532**, WHO, Geneva (1973).
9. E. Somer, Toxic potential of trace metals in foods. *A rev. J. Food Sci.*, **39**, 215 (1974).
10. R. F. Guerrero, A. Liazid, M. B. Palma, R. Puertas, G. Barrio, A. G. Izquierdo, C. G. Barroso, E. C. Villar. Phenolic characterization of red grapes autochthonous to Andalusia. *Food Chem.*, **112**, 949 (2009).
11. A. Lončarić, A. Pichler, I. Trtinjak, V. Pilizota and M. Kopjar, *LWT – Food. Sci and Tech.*, **73**, 391 (2016).
12. V. C Bochi, M. T Barcia, D. Rodrigues, C. S Speroni, M. M. Giusti, H. T Godoy. Polyphenol extraction optimization from Ceylon gooseberry (*Dovyalis hebecarpa*) pulp. *Food Chem.*, **164**, 347 (2014).
13. J. Zhiy, L. R. Howard, Subcritical Water and Sulfured Water Extraction of Anthocyanins and Other Phenolics from Dried Red Grape Skin, *J. of Food Sci.*, **70**, S 270 (2005).
14. M. Scordino, A. D. Mauro, A. Passerini and E. Maccarone, Adsorption of flavonoids on resins: Hesperidin. *J. of Agri. and Food Chem.*, **51**, 6998 (2003).
15. B. Fu, J. Liu, H. Li, L. Li. F Lee. S. C. and X. Wang., The application of macroporous resins in the separation of licorice flavonoids and glycyrrhizic acid. *J. of Chrom. A.*, **1089**, 18 (2005).
16. M. Ahmaruzzaman, Adsorption of phenolic compounds on low-cost adsorbents: a review. *Adv. Collo. Inter. Sci.*, **84**, 48 (2001).
17. K. Nakagawa, A. Namba, S. R. Mukai, H. Tamon, P. Ariyadejwanich, W. Tanthapanichakoon.: Adsorption of phenol and reactive dye from aqueous solution on activated carbons derived from solid wastes. *Wat. Res.*, **38**, 1791 (2004).
18. F. Su, L. Lv, T.M Hui, X.S Zhao: Phenol adsorption on zeolite-templated carbons with different structural and surface properties. *Carb.*, **43**, 1156 (2005).
19. A. P Terzyk, Further insights into the role of carbon surface functionalities in the mechanism of phenol adsorption. *J Collo. Inter. Sci.*, **268**, 301 (2003).
20. Y. and A.H. Aydin. New Method for Measurement of Surface Areas of Microleakage at the Primary Teeth by Biomolecule Characteristics of Methylene Blue. *Biotech & Biote. Eq.*, **18119** (2014).
21. O. Komatsu, H. Nishida et al. Application of titanium dioxide nanotubes to tooth whitening. Koma. et al., *Nano. Bio.*, **6**, **63** (2014).
22. A. A. Taha, A. M. Ahmed, H. H. Abdel Rahman, F. M. Abouzeid & M. O. Abdel, Maksou, Removal of Nickel Ions by Adsorption on Nano Bentonite: Equilibrium, Kinetic and Thermodynamics. *J. of Disp. Sci and Tech.*, **38**, **767** (2017).
23. P. Pandey, S. Sharma, S. Sami Kinetics and Equilibrium Study of Chromium Adsorption on ZeoliteNaX, *Inter. J. of Envi. Sci. and Tech.*, **7**, 395. (2010).
24. M. Martínez, N. Miralles, S Hidalgo, N. Fiol, I. Villaescusa, and J. Poch, Removal of Lead and Cadmium from Aqueous Solution Using Grape Stalk Waste. *J. of Haz. Mater.*, **133**, 203 (2006).
25. M. Turabik, B Gozmen, Removal of basic textile dyes in single and multi-dye solutions by adsorption: statistical optimization and equilibrium isotherm studies. *Cle. Soil Air Wat.*, **41**:1080 (2013).
26. I. Langmuir, the Constitution and Fundamental Properties of Solids and Liquids. *J. of the Ame. Chem. Soc.*, **38**, 2221 (1916).
27. M Hema. and S. Arivoli, Adsorption Kinetics and Thermodynamics of Malachite Green Dye onto Acid Activated Low Cost Carbon. *J. of App. Sci. and Env.Man.*, **12**, **43** (2008).
28. K. R. Hall, L. C. Eagleton, A. Acrivos and T. Vermeulen, "Pore and Solid Diffusion Kinetics in Fixed Bed Adsorption under Constant Pattern Conditions," *Ind & Eng. Chem. Fund.*, Vol. **5**, **212** (1966).
29. H. M. F. Freundlich, "Over the Adsorption in Solution," *The J. of Phy. Chem.*, **57**, 385 (1906).
30. A.K. Meena., C. R Kiran., and G. K. Mishra., Removal of Heavy Metal Ions from Aqueous Solutions Using Chemically (Na₂S) Treated Granular Activated Carbon as an Adsorbent. *J. of Sci. and Ind. Res.*, **69**, 449 (2010).
31. S. M. Hasany, M. M Saeed, and M. Ahmed., Sorption and Thermodynamic Behavior of Zinc (II)-Thiocyanate Complexes onto Polyurethane Foam from Acidic Solutions. *J. of Rad. and Nuc. Chem.*, **252**, 477 (2002).
32. Y. S., Citation review of Lagergren kinetic rate equation on adsorption reactions, *Scien.*, **59** 171 (2004).

33. S. Lagergren, About the Theory of So-Called Adsorption of Soluble Substance. *Kun.Sve. Vete.n. Hand.*, **24**, 1 (1898).
34. Y. S .Ho, Review of second-order models for adsorption systems, *J. of Haz. Mat.*, B **136**, 681 (2006).
35. Y.S .Ho and, G. McKay., Sorption of Dye from Aqueous Solution by Peat. *Chem.Eng. J.*, **70**, 115 (1998).
36. E. Guibal, C. Milot, and J. M. Tobin, "Metal-anion sorption by chitosan beads: equilibrium and kinetic studies," *Ind. and Eng. Chem. Res.*, **37**, 1454 (1998).
37. M. Dog˘an, O˘ zdemir Y, M Alkan Adsorption kinetics and mechanism of cationic methyl violet and methylene blue dyes onto sepiolite. *Dye Pig. Fig.* **75**, 701 (2007).
38. B. Kocadagistan, E. Kocadagistan, The effects of sunflower seed shell modifying process on textile dye adsorption: kinetic, thermodynamic and equilibrium study. *Des. Wat Tre.*, **57**, 3168 (2016).
39. Y.S Ho and G. McKay, Pseudo-Second Order Model for Sorption Processes. *Pro. Bio.*, **34**, 451 (1999).
40. D.E Akretche, Metals Removal from Industrial Effluents. In: Coca-Prados, J. and Gutierrez-Cervello, G., Eds., *Water Purification and Management, Spr. Sci .Bus. Med. BV, Alg.*, **95** (2011).
41. A. A. Atia, A. M. Donia, and A. M. Yousif, "Removal of some hazardous heavy metals from aqueous solution using magnetic chelating resin with iminodiacetate functionality," *Sep. and Pur. Tech.*, **61**, 348 (2008)
42. E. Guibal, C. Milot, and J. M. Tobin, "Metal-anion sorption by chitosan beads: equilibrium and kinetic studies," *Ind. and Eng. Chem. Res.*, **37**, 1454 (1998).
43. I A. W Tan and B. Hameed, Adsorption Isotherms, Kinetics, Thermodynamics and Desorption Studies of Basic Dye on Activated Carbon Derived from Oil Palm Empty Fruit Bunch. *J. of App. Sci.*, **10**, 2565 (2010).
44. B. H Aregawi and A.A Mengistie, Removal of Ni (II) from Aqueous Solution Using Leaf, Bark and Seed of Moringa stenopetala Adsorbents. *Bull of the Chem. Soc. of Ethio.*, **27**, 35 (2013).
45. A. Peter, J. Paula, Physical Chemistry. Oxford University pres, p.7167 (2006).
46. I. A.W Tan and B. Hameed, Adsorption Isotherms, Kinetics, Thermodynamics and Desorption Studies of Basic Dye on Activated Carbon Derived from Oil Palm Empty Fruit Bunch. *J. of App. Sci.*, **10**, 2565 (2010).
47. Y. S .Ho, Review of second-order models for adsorption systems, *J.of Haz. Mat.*, **136**, 681 (2006).
48. Y.S .Ho and, G. McKay, Sorption of Dye from Aqueous Solution by Peat. *Chem.Eng.J.*, **70**, 115 (1998).
49. E. Guibal, C. Milot, and J. M. Tobin, "Metal-anion sorption by chitosan beads: equilibrium and kinetic studies," *Ind. and Eng. Chem. Res.*, **37**, 1454 (1998).
50. M. Dog˘an, O. zdemir Y, M Alkan Adsorption kinetics and mechanism of cationic methyl violet and methylene blue dyes onto sepiolite. *Dye Pig.* **75**, 701 (2007).
51. B. Kocadagistan, E. Kocadagistan, The effects of sunflower seed shell modifying process on textile dye adsorption: kinetic, thermodynamic and equilibrium study. *Des. Wat. Trea.*, **57**, 3168 (2016).
52. Y.S Ho, and G. McKay, Pseudo-Second Order Model for Sorption Processes. *Pro. Bio.*, **34**, 451 (1999).
53. D.E Akretche, Metals Removal from Industrial Effluents. In: Coca-Prados, J. and Gutierrez-Cervello, G., Eds., *Water Purification and Management, Spr. Sci. Bus Med. BV, Alg.*, **95**-117 (2011).
54. A. A. Atia, A. M. Donia, and A. M. Yousif, "Removal of some hazardous heavy metals from aqueous solution using magnetic chelating resin with iminodiacetate functionality," *Sep. and Pur. Tech.*, **61**, 348 (2008)
55. E. Guibal, C. Milot, and J. M. Tobin, "Metal-anion sorption by chitosan beads: equilibrium and kinetic studies," *Ind. and Eng. Chem. Res.*, vol., **1454** (1998).
56. I. A.W Tan and B. Hameed, Adsorption Isotherms, Kinetics, Thermodynamics and Desorption Studies of Basic Dye on Activated Carbon Derived from Oil Palm Empty Fruit Bunch. *J. of App. Sci.*, **10**, 2565 (2010).
57. B.H Aregawi and A.A Mengistie, Removal of Ni (II) from Aqueous Solution Using Leaf, Bark and Seed of Moringa stenopetala Adsorbents. *Bul. of the Chem. Soc. of Eth.*, **27**, 35 (2013)
58. A. Peter, J. Paula, Physical Chemistry. Oxford University. **p.7167** (2006).
59. I. A.W Tan. and B. Hameed, Adsorption Isotherms, Kinetics, Thermodynamics and Desorption Studies of Basic Dye on Activated Carbon Derived from Oil Palm Empty Fruit Bunch. *J. of App. Sci.*, **10**, 2565 (2010).